Hybrid Railway Power Conditioner With Partial Compensation for Converter Rating Reduction

Ning Yi Dai, *Member, IEEE*, Keng-Weng Lao, *Student Member, IEEE*, and Chi-Seng Lam, *Member, IEEE*

***Abstract*—Single-phase traction transformers are widely used in traction power supply systems due to their characteristics such as a low cost and a simple structure. Railway power conditioners (RPCs) could increase the loading capacity of substations and improve the supply quality. In this paper, a hybrid RPC (HRPC) is applied to reduce reactive power, relieve system unbalance, and suppress harmonics. The operational voltage of the HRPC is much lower than that of a conventional RPC. A method named partial compensation was used to reduce the current rating of the RPC, in which the compensating currents are expressed as a function of the power factor target at the grid side. When this method is used in the HPRC, the operational voltage varies with the compensating currents over a wide range. A comprehensive design procedure is proposed so that both the current and voltage ratings of the HRPC are reduced with partial compensation. A reduction of more than 50% is achieved by compensating the power factor at the grid side to 0.95 instead of to unity. The control block diagram for the HRPC with partial compensation is presented. The design and control of the HRPC are validated by simulation and experimental results.**

***Index Terms*—Power conditioning, power conversion, power filter, power quality, rail transportation power system.**

I. Introduction

RAILWAY electrification systems play an essential role in modern transportation systems. Different systems are used for urban and intercity areas. The AC system is adopted in the USA, China, India, and France for long-distance railways [1], [2]. The configuration of a single-phase 25-kV traction power supply system is shown in Fig. 1.

Traction substations are equipped with transformers and provide power to electric locomotives. Single-phase traction transformers are widely used due to their characteristics such as a low cost and a simple structure [3]–[5]. As shown in Fig. 1, single-phase transformers are alternatively connected to the three phases to reduce current unbalance. However, unbalance is still a severe problem at the grid side since traction loads are not evenly distributed among each section [6], [7]. Furthermore, electric locomotives inject reactive power and harmonics to the traction power supply system, causing the traction transformer to work in a derating mode and increasing system losses [8]–[10].

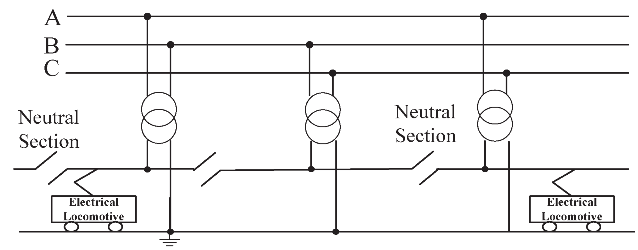

Fig. 1. Traction power supply system using single-phase traction transformers.

Railway power conditioners (RPCs) or various power quality compensators are developed to solve these problems. A static var compensator (SVC) was used [11], [12]. However, the dynamic performance of the SVC is poor, and the system occupies a large physical area. Compared with the SVC, an active power filter (APF) or a static synchronous compensator (STATCOM) has several advantages, such as a fast response, high efficiency, and a low harmonic output [13], [14]. Single-phase APFs are used to compensate for the harmonics and the reactive power, but they are not able to reduce the grid-side current unbalance [15], [16]. An RPC was developed for the traction power supply system, which uses traction transformers with two secondary windings, such as a V/V transformer or a Scott transformer [14], [17]. The main circuit of the RPC is a single-phase back-to-back converter, and it is able to compensate for the current unbalance, the reactive power, and the harmonics simultaneously [17]–[19]. The RPC was also used to develop a new traction power supply mode, i.e., a cophase traction power supply system. One cophase traction power system is now operating in the Meishan traction substation in China.

The main disadvantage of the RPC and the cophase traction power supply system is a high converter rating and its correspondingly high cost. According to the field-recorded data [20], traction loads vary from 0 to around 40 MW. A previous study indicates that the RPC needs to transfer half of the load active power and provide all of the reactive power. Hence, the rating of the back-to-back converter in the RPC is high. A hybrid

Manuscript received November 11, 2014; revised March 11, 2015; accepted April 8, 2015. Date of publication April 24, 2015; date of current version September 16, 2015. Paper 2014-TSC-0803.R1, presented at the 2014 IEEE Energy Conversion Congress and Exposition, Pittsburgh, PA, USA, September 20–24, and approved for publication in the IEEE Transactions on Industry Applications by the Transportation Systems Committee of the IEEE Industry Applications Society. This work was supported in part by the Science and Technology Development Fund of the Macau Special Administrative Region Government under Project 015/2008/A1 and in part by the University of Macau under Project MYRG2014-00024-FST.

N. Y. Dai and K.-W. Lao are with the Department of Electrical and Computer Engineering, Faculty of Science and Technology, University of Macau, Macau 999078, China (e-mail: nydai@umac.mo; kwlaojohnny@gmail.com).

C.-S. Lam is with the State Key Laboratory of Analog and Mixed-Signal VLSI, Faculty of Science and Technology, University of Macau, Macau 999078, China (e-mail: cslam@umac.mo).

Color versions of one or more of the figures in this paper are available online at http://ieeexplore.ieee.org.

Digital Object Identifier 10.1109/TIA.2015.2426134

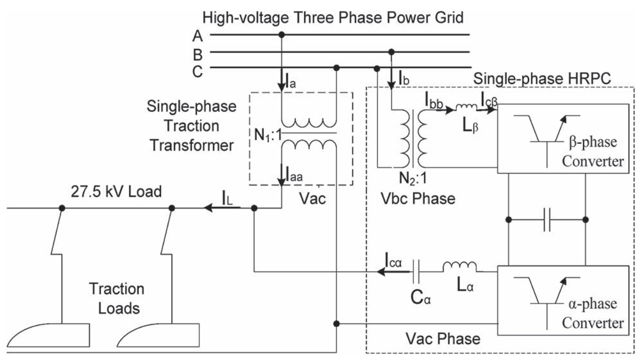

Fig. 2. Traction power supply with a single-phase HPRC.

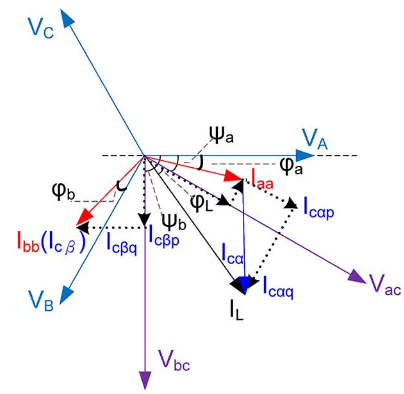

Fig. 3. Phasor diagram of the traction power supply system with the HRPC.

RPC (HRPC) was proposed as a low-cost alternative to the RPC in the cophase traction power supply system [21]–[23]. By inserting a capacitor in one coupling branch, its operational voltage is significantly reduced compared with that of the RPC. Therefore, a lower dc-link voltage is set for the back-to-back converter, which reduces its rating and the running losses of the HRPC.

In China, the supply system of recently built high-speed railways still mainly uses single-phase traction transformers. In order to satisfy the standard of power quality, traction substations are connected to a 500-kV network to get sufficient short-circuit capacity [5]. At the same time, a number of existing traction substations are facing the challenges of increasing loading and deteriorated power quality. In this paper, the HRPC is applied to the traction power supply system in Fig. 1. The system configuration is shown in Fig. 2. The capacitive coupling phase of the HRPC is connected to the secondary side of the traction transformer. The other phase is connected to the high-voltage power grid. The power conditioning capability of the HRPC is used to reduce the reactive power, relieve the system unbalance, and suppress the harmonics. More importantly, the HRPC is able to increase the loading capacity of the substation by transferring power from the three-phase power grid to supply the traction loads. This is extremely useful for substations with insufficient loading capacity.

In contrast to the cophase traction power supply system, conventional traction power supply systems allow a certain amount of unbalanced and/or distorted currents flowing in the system. The higher the short-circuit capacity of the system is, the more it is able to maintain its voltage in case of a current distortion. Hence, power conditioners are used to improve the power factor or reduce the current unbalance instead of fully solving the problems. Partial compensation is a more economical solution, and it was introduced in [24], in which the compensating currents are expressed as a function of the power factor at the grid side. The current rating of the RPC was effectively reduced with partial compensation, but its voltage rating is kept the same [24].

Partial compensation is applied to reduce both the current and voltage ratings of the converter in the HPRC in this paper. The operational voltage of the HRPC varies with the compensating currents over a wide range. Not only the current rating but also the dc-link voltage and the coupling impedance need to be redesigned for the HRPC under partial compensation. In Section II, the current and voltage ratings of the HRPC with partial compensation are first analyzed. The impact of the compensating current variation on the converter rating of the HRPC is assessed. The selection of partial compensation parameters is discussed in Section III, where a comprehensive design procedure and the control block diagram are also provided. Simulation verification and experimental verification are provided in Sections IV and V, respectively.

II. HRPC Rating Reduction With Partial Compensation

A. Compensating Current Calculation

The configuration of the traction power supply system with a single-phase HRPC is given in Fig. 2. Based on its fundamental frequency model, a phasor diagram is shown in Fig. 3. The voltages at the high-voltage grid side are denoted as V_A, V_B, and V_C, whereas the secondary-side voltages of the single-phase transformer are expressed as $V_{\rm ac}$ and V_{bc}. The main circuit of the HRPC is a back-to-back converter, which absorbs power from the V_{bc} phase and injects power into the $V_{\rm ac}$ phase. The converter connecting to the $V_{\rm ac}$ phase is named the α-phase converter, and the converter connecting to the V_{bc} phase is named the β-phase converter. The output currents of these two converters are denoted as $I_{c\alpha}$ and $I_{c\beta}$, respectively. The load current is I_L, and its power factor is $\cos(\varphi_L)$. The currents at the grid side are

$$\begin{bmatrix}\dot{I}_a\\ \dot{I}_b\\ \dot{I}_c\end{bmatrix} = \begin{bmatrix}\dot{I}_{aa}e^{-j\psi_a}/N_1\\ \dot{I}_{bb}e^{-j\psi_b}/N_2\\ -\dot{I}_a-\dot{I}_b\end{bmatrix} = \begin{bmatrix}(\dot{I}_L-\dot{I}_{c\alpha})e^{-j\psi_a}/N_1\\ \dot{I}_{c\beta}e^{-j\psi_b}/N_2\\ -\dot{I}_a-\dot{I}_b\end{bmatrix} \quad (1)$$

where N_1 is the ratio of the turns of the single-phase traction transformer, N_2 is the ratio of the turns of the coupling transformer at the V_{bc} phase, $\psi_a = \pi/6$, and $\psi_b = \pi/2$.

Full compensation is defined as the case in which the currents on the grid side are balanced with a unity power factor. The required rating of the power converters in this case is used as the benchmark to measure the converter ratings with partial compensation. Subscript f is used to denote the parameters related to full compensation. The corresponding reference current of the HRPC for achieving full compensation is given in [24]

$$\begin{bmatrix} I_{c\alpha p\_f} \\ I_{c\alpha q\_f} \\ I_{c\beta p\_f} \\ I_{c\beta q\_f} \end{bmatrix} = \begin{bmatrix} \frac{1}{2} \cdot I_{Lp} \\ \tan(\varphi_L) I_{Lp} + \frac{\tan(\psi_a)}{2} I_{Lp} \\ \frac{N_2}{N_1} \cdot \frac{1}{2} I_{Lp} \\ \frac{N_2}{N_1} \cdot \tan\left(\frac{2}{3}\pi - \psi_b\right) \cdot \frac{1}{2} I_{Lp} \end{bmatrix}. \quad (2)$$

Subscript p indicates a current that is in phase with the supply voltage, and subscript q indicates a current that is orthogonal to the voltage. The expression of I_{Lp} is given in

$$I_{Lp} = I_L \cdot \cos\varphi_L. \quad (3)$$

The current ratings of the α-phase converter and the β-phase converter with full compensation are expressed as follows:

$$I_{c\alpha\_f} = \sqrt{\left(\frac{1}{2}\right)^2 + \left(\tan(\varphi_L) + \frac{\tan(\psi_a)}{2}\right)^2} I_{Lp} \quad (4)$$

$$I_{c\beta\_f} = \sqrt{\left(\frac{1}{2}\right)^2 + \left(\frac{\tan\left(\frac{2}{3}\pi - \psi_b\right)}{2}\right)^2} \cdot \frac{N_2}{N_1} \cdot I_{Lp}. \quad (5)$$

B. Current Rating With Partial Compensation

According to (2), the HRPC transfers half of the load active power under full compensation. A parameter k is introduced to modify the percentage of the load active power supplied by the HRPC. It also affects the reactive power being injected into the supply system because the power factor is the ratio between the active power and the reactive power. Two more parameters, i.e., phase angles φ_a and φ_b, are used to modify the reactive power under partial compensation. They are obtained from the power factor at the corresponding phase after the HRPC operates. Hence, the reference currents in (2) are revised to the following with partial compensation [24]:

$$\begin{bmatrix} I_{c\alpha p} \\ I_{c\alpha q} \\ I_{c\beta p} \\ I_{c\beta q} \end{bmatrix} = \begin{bmatrix} k \cdot I_{Lp} \\ \tan(\varphi_L) I_{Lp} + \tan(\psi_a - \varphi_a)(1-k) I_{Lp} \\ \frac{N_2}{N_1} \cdot k \cdot I_{Lp} \\ \tan\left(\frac{2}{3}\pi - \psi_b + \varphi_b\right) \frac{N_2}{N_1} \cdot k \cdot I_{Lp} \end{bmatrix}. \quad (6)$$

The current ratings of the two converters in the HRPC with partial compensation are expressed as follows:

$$I_{c\alpha} = \sqrt{k^2 + (\tan(\varphi_L) + \tan(\psi_a - \varphi_a)(1-k))^2} I_{Lp} \quad (7)$$

$$I_{c\beta} = \sqrt{(k)^2 + \left(\tan\left(\frac{2}{3}\pi - \psi_b + \varphi_b\right) \cdot k\right)^2} \cdot \frac{N_2}{N_1} \cdot I_{Lp}. \quad (8)$$

It is assumed that the load power factor is 0.85. The current ratings' variation in terms of the power factor and k is shown in Fig. 4. The ratings in Fig. 4 are normalized by dividing the rating by that required for full compensation. It is concluded in Fig. 4 that the current rating of the α-phase converter does not linearly vary with k. There is one minimum point for each selected power factor target at phase A. The current rating of the

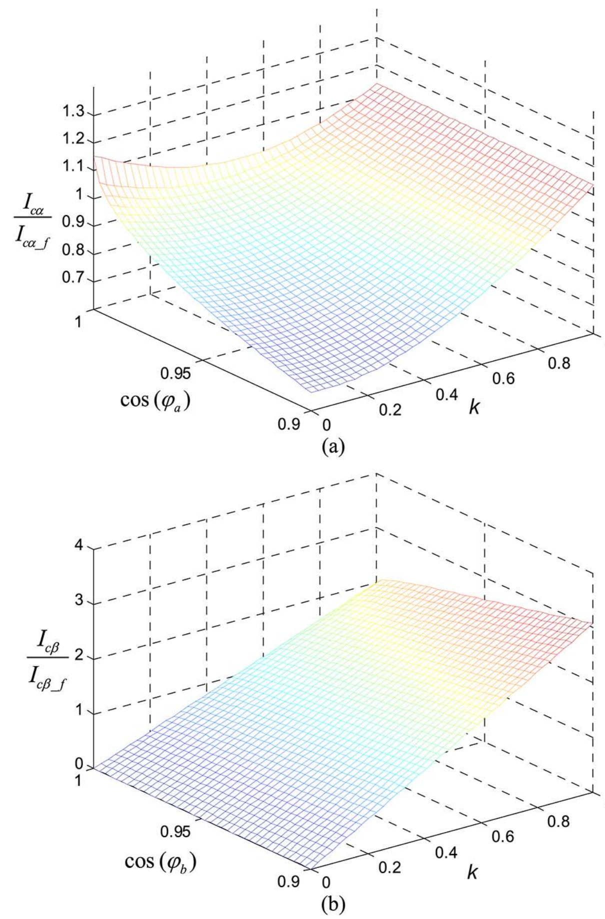

Fig. 4. Current ratings. (a) α-phase converter. (b) β-phase converter.

β-phase converter linearly varies with k. When the power factor is lower than 1 and an appropriate value is selected for k, the current rating reduction is achieved with partial compensation.

C. Voltage Ratings With Partial Compensation

In this section, the voltage ratings of the power converters in the HRPC are calculated when partial compensation is applied. The output voltage of the α-phase converter and its rating are expressed as follows:

$$\vec{V}_{\text{inv}\alpha} = \vec{V}_{\text{ac}} + \vec{V}_{LC} = \vec{V}_{\text{ac}} - jX_{LC} \cdot \vec{i}_{c\alpha} \quad (9)$$

$$V_{\text{inv}\alpha} = \sqrt{(V_{\text{ac}} - I_{c\alpha q} X_{LC})^2 + (I_{c\alpha p} X_{LC})^2}. \quad (10)$$

For a fixed compensating current, the optimum parameter selection of coupling impedance X_{LC} is achieved by taking the derivative of (10) with X_{LC} and setting it to zero. The process and results are shown in

$$\frac{d(V_{\text{inv}\alpha}^2)}{d(X_{LC})} = 2V_{\text{ac}} I_{c\alpha q} + 2(I_{c\alpha q}^2 + I_{c\alpha p}^2) X_{LC} = 0 \quad (11)$$

$$X_{LC} = \frac{\tan(\varphi_L) + \tan(\psi_a - \varphi_a)(1-k)}{((\tan(\varphi_L) + \tan(\psi_a - \varphi_a)(1-k))^2 + k^2} \cdot \frac{V_{\text{ac}}}{I_{Lp}}. \quad (12)$$

By substituting (7) and (12) into (10), the voltage rating of the α-phase converter is deduced as

$$V_{\mathrm{inv}\alpha} = \frac{k}{\sqrt{\left(\tan(\varphi_L) + \tan(\psi_a - \varphi_a)(1-k)\right)^2 + k^2}} \cdot V_{\mathrm{ac}}. \tag{13}$$

The voltage rating with full compensation is given as

$$V_{\mathrm{inv}\alpha\_f} = \frac{\frac{1}{2}}{\sqrt{\left(\tan(\varphi_L) + \tan(\psi_a)\left(\frac{1}{2}\right)\right)^2 + \left(\frac{1}{2}\right)^2}} \cdot V_{\mathrm{ac}}. \tag{14}$$

The output voltage of the β-phase converter and its rating are expressed as follows:

$$\vec{V}_{\mathrm{inv}\beta} = \vec{V}_{bc} - \vec{V}_L = \vec{V}_{bc} - jX_L \cdot \vec{i}_{c\beta} \tag{15}$$

$$V_{\mathrm{inv}\beta} = \sqrt{(V_{bc} - I_{c\beta q}X_L)^2 + (I_{c\beta p}X_L)^2}. \tag{16}$$

The coupling inductor of the β-phase converter is selected to suppress the output current ripple and is kept as small as possible. Its value is assumed to be

$$X_L = m \cdot \frac{V_{bc}}{\left(\frac{N_2}{N_1}\right) I_{Lp}}. \tag{17}$$

By substituting (6) and (17) into (16), the voltage rating of the β-phase converter is given with partial compensation and full compensation, respectively, in the following:

$$V_{\mathrm{inv}\beta} = \sqrt{\left(1 - \tan\left(\frac{2}{3}\pi - \psi_b + \varphi_b\right) \cdot m \cdot k\right)^2 + k^2 \cdot m^2} \cdot V_{bc} \tag{18}$$

$$V_{\mathrm{inv}\beta\_f} = \sqrt{\left(1 - \frac{1}{2}\tan\left(\frac{2}{3}\pi - \psi_b\right) \cdot m\right)^2 + \frac{1}{4} \cdot m^2} \cdot V_{bc}. \tag{19}$$

The variations in the voltage rating in terms of the power factor and k are illustrated in Fig. 5. The voltage rating of the α-phase converter varies over a wide range with partial compensation. Coefficient m is set to 10% when the voltage ratings are calculated in Fig. 5(b). In contrast to the voltage rating of the α-phase converter, the voltage rating of the β-phase converter varies over a narrower range. The reason is that the variation in the voltage crossing the coupling impedance is higher at the α-phase converter than at the β-phase converter. When the power factor is lower than 1 and an appropriate value is selected for k, the voltage rating reduction is also achieved with partial compensation. In summary, the voltage rating needs to be adjusted together with the current rating in the HRPC. However, it is not the case in the RPC when partial compensation is implemented.

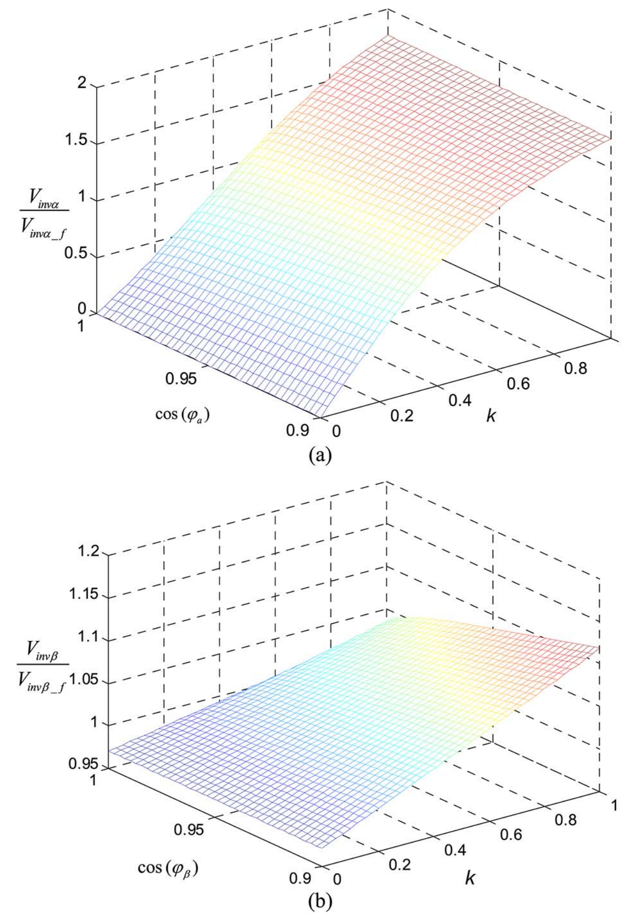

Fig. 5. Voltage ratings. (a) α-phase converter. (b) β-phase converter.

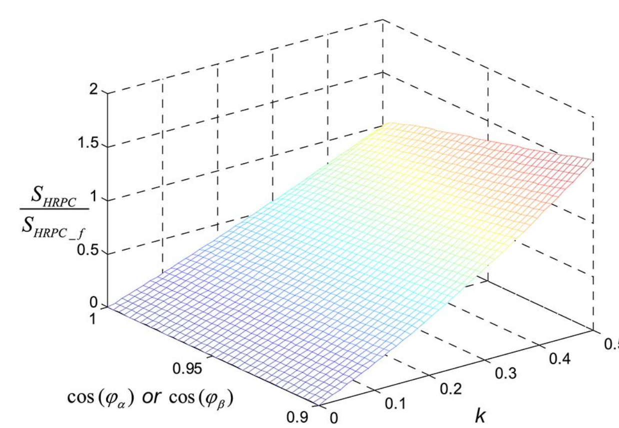

Fig. 6. Variation in the converter rating in terms of the power factor and k.

D. HRPC Rating Under Partial Compensation

In this section, the rating of the power converters in the HRPC is calculated as follows:

$$S_{\mathrm{HRPC}} = S_\alpha + S_\beta = V_{\mathrm{inv}\alpha} \cdot I_{c\alpha} + V_{\mathrm{inv}\beta} \cdot I_{c\beta}. \tag{20}$$

It is assumed that $\cos(\varphi_a) = \cos(\varphi_b)$. The variation in the converter rating in terms of the power factor and k is shown in Fig. 6.

III. System Design and Implementation

A. Parameter Selection for Partial Compensation

As illustrated in Fig. 6, designing with partial compensation can significantly reduce the rating of the power converters.

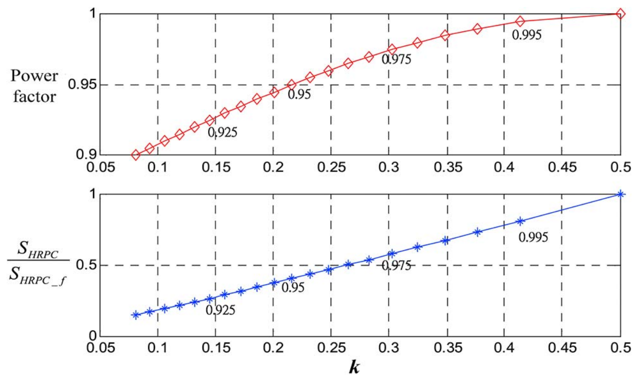

Fig. 7. Effects of k on the power factor and the HRPC rating.

However, the power factor at the grid side is not able to reach unity under partial compensation. The variation in the compensating current also affects the performance of current balancing. There is a tradeoff between the HRPC rating reduction and the power conditioning performance.

There are three parameters affecting the compensating currents in (6), i.e., k, φ_a, and φ_b. The last two parameters are determined by the grid-side power factor. There is a relationship between parameter k and the grid-side power factor, as given in (21), shown at the bottom of the page [24].

To reach the same grid-side power factor, the phase angle of each phase could be either leading or legging. The k value varies in terms of the phase angle for each phase. A previous study verified that the minimum current rating is obtained by setting the power angle of phases A and B as lagging and setting the power angle of phase C as leading under partial compensation [24] This scheme is also used in this paper to design the HRPC with partial compensation.

The effects of the k value on the grid-side power factor and the HRPC rating are shown in Fig. 7. The HRPC rating almost linearly decreases with k. The k value decreases much faster when the power factor is close to unity. The HRPC rating has a reduction of about 20% by setting the power factor to 0.995 instead of 1. As a result, partial compensation can achieve HRPC rating reduction without sacrificing the system performance too much.

B. Comprehensive Design Procedure of HRPC

With the selected power factor and k, the coupling impedance and dc-link voltage of the HRPC need to be adjusted accordingly. The comprehensive design procedure of the HRPC is presented as follows.

1) Set the power factor target at the grid side after the HRPC operates as follows:

$$\mathrm{PF_{grid}} = \frac{(P_A + P_B + P_C)}{(S_A + S_B + S_C)}. \tag{22}$$

2) Partial compensation coefficient k is calculated by (23), shown at the bottom of the page.

3) The reference currents for controlling the HRPC are given in the following, in which $k_\alpha = \tan(\psi_a - \varphi_a)(1-k)$ and $k_\beta = \tan((2/3)\pi - \psi_b + \varphi_b)$:

$$\begin{bmatrix} I_{c\alpha p} \\ I_{c\alpha q} \\ I_{c\beta p} \\ I_{c\beta q} \end{bmatrix} = \begin{bmatrix} k \cdot I_{Lp} \\ \tan(\varphi_L) I_{Lp} + \tan(\psi_a - \varphi_a)(1-k) I_{Lp} \\ \frac{N_2}{N_1} \cdot k \cdot I_{Lp} \\ \tan\left(\frac{2}{3}\pi - \psi_b + \varphi_b\right) \frac{N_2}{N_1} \cdot k \cdot I_{Lp} \end{bmatrix} = \begin{bmatrix} k \cdot I_{Lp} \\ \tan(\varphi_L) I_{Lp} + k_\alpha I_{Lp} \\ \frac{N_2}{N_1} \cdot k \cdot I_{Lp} \\ \frac{N_2}{N_1} \cdot k_\beta \cdot k \cdot I_{Lp} \end{bmatrix}. \tag{24}$$

4) Calculate the coupling impedance of the α-phase converter as follows:

$$X_{LC} = \frac{\tan(\varphi_L) + \tan(\psi_a - \varphi_a)(1-k)}{((\tan(\varphi_L) + \tan(\psi_a - \varphi_a)(1-k))^2 + k^2} \cdot \frac{V_{\mathrm{ac}}}{I_{Lp}}. \tag{25}$$

5) Calculate the α-phase coupling inductor and capacitor taking the harmonic compensation into consideration. The load harmonic current at the hth harmonic is assumed to be r_h times the fundamental value, as given in

$$I_{Lh} = r_h \cdot I_{L1} = r_h \cdot I_{L1p} / \cos(\varphi_L). \tag{26}$$

The coupling impedance is selected to minimize the harmonic operational voltage, as given in the

$$k = \frac{\cos\left(\psi_b - \varphi_b - \frac{2}{3}\pi\right) \sin\left(\varphi_a - \varphi_c + \frac{2}{3}\pi\right)}{\cos\left(\psi_b - \varphi_b - \frac{2}{3}\pi\right) \sin\left(\phi_a - \varphi_c + \frac{2}{3}\pi\right) + \cos(\psi_a - \varphi_a) \sin\left(\varphi_c - \varphi_b + \frac{2}{3}\pi\right)} \tag{21}$$

$$\begin{aligned} k &= \frac{\cos\left(\psi_b - \varphi_b - \frac{2}{3}\pi\right) \sin\left(\varphi_a - \varphi_c + \frac{2}{3}\pi\right)}{\cos\left(\psi_b - \varphi_b - \frac{2}{3}\pi\right) \sin\left(\varphi_a - \varphi_c + \frac{2}{3}\pi\right) + \cos(\psi_a - \varphi_a) \sin\left(\varphi_c - \varphi_b + \frac{2}{3}\pi\right)} \\ \varphi_a &= \varphi_b = -\varphi_c = a\cos(\mathrm{PF_{grid}}). \end{aligned} \tag{23}$$

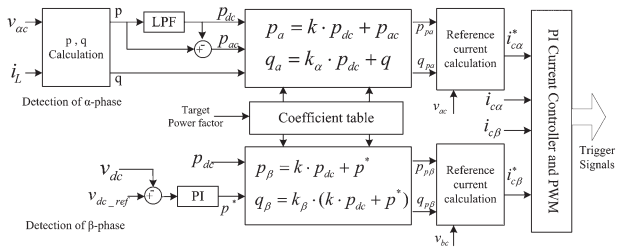

Fig. 8. Control system of the HRPC.

following [23]:

$$L_a = \frac{\frac{\sum_{h=2}^{\infty}(r_h)^2 \cdot \frac{2(h^2-1)}{h^2}}{\sum_{h=2}^{\infty}(r_h)^2 \cdot \frac{2(h^2-1)^2}{h^2}}}{\omega_1} X_{LC} = \frac{k_L}{\omega_1} X_{LC} \tag{27}$$

$$C_a = \frac{1}{\omega_1\left(1 + \frac{\sum_{h=2}^{\infty}(r_h)^2 \cdot \frac{2(h^2-1)}{h^2}}{\sum_{h=2}^{\infty}(r_h)^2 \cdot \frac{2(h^2-1)^2}{h^2}}\right) \cdot X_{LCa}} = \frac{1}{\omega_1 k_c \cdot X_{LC}}. \tag{28}$$

6) Calculate the β-phase coupling inductor according to (17) and the following:

$$L_\beta = \frac{X_L}{\omega_1}. \tag{29}$$

7) Determine the dc-link operation voltage in the HRPC as follows:

$$V_{\rm dc} = \sqrt{2}\sqrt{V_{\rm inv\alpha}^2 + \sum_{h=2}^{\infty}(X_{LCh} \cdot I_{Lh})^2} \tag{30}$$

where $X_{LCh} = -(1/h)[(h^2-1)k_L - 1]X_{LC}$.

8) The α-phase and β-phase converters are connected to the same dc bus. However, the operational voltage at the β-phase converter is much higher than that at the α-phase converter. The problem is solved by adjusting the ratio of the turns of the coupling transformer at the β-phase converter. It is expressed as follows:

$$N_2 = \frac{V_{BC}}{V_{\rm dc}/\sqrt{2}}. \tag{31}$$

C. Control System of HRPC

Fig. 8 illustrates the control diagram of the HRPC. The single-phase instantaneous theory is used to calculate the power of the traction loads. The instantaneous active power and reactive power are calculated as follows, in which $v_{\alpha d}$ and $i_{\alpha d}$ are the 90° delays of the system voltage and the load current, respectively,

$$\begin{bmatrix} p \\ q \end{bmatrix} = \begin{bmatrix} v_\alpha \cdot i_L + v_{\alpha d} \cdot i_{Ld} \\ v_\alpha \cdot i_{Ld} - v_{\alpha d} \cdot i_L \end{bmatrix}. \tag{32}$$

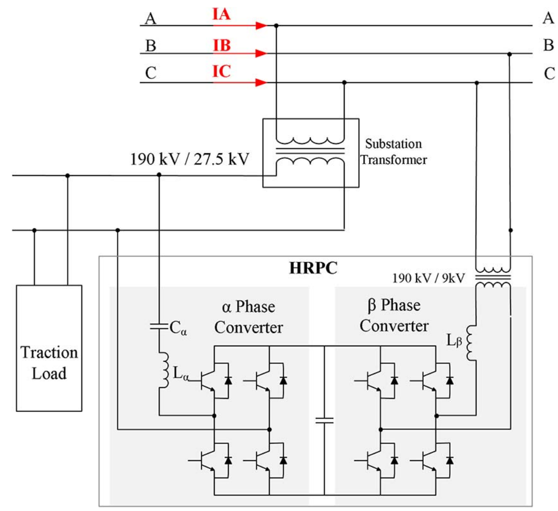

Fig. 9. System configuration.

TABLE I
ON-SITE STATISTICS FOR THE HARMONIC CURRENT CONTENTS IN THE WUQING SUBSTATION'S TRACTION LOAD

	3rd	5th	7th	9th	11th
Harmonic contents (% of fundamental)	10.81	7.96	4.51	3.04	2.68

Instead of calculating the compensating current by using (24), partial compensation is achieved by multiplying the corresponding coefficient to the power reference, as given in

$$\begin{bmatrix} p_{p\alpha} \\ q_{p\alpha} \\ p_{p\beta} \\ q_{p\beta} \end{bmatrix} = \begin{bmatrix} k \cdot p_{\rm dc} + p_{\rm ac} \\ k_\alpha \cdot p_{\rm dc} + q \\ k \cdot p_{\rm dc} + p^* \\ k_\beta \cdot (p_{\rm dc} \cdot k + p^*) \end{bmatrix}. \tag{33}$$

By varying these coefficients, the HRPC is able to improve the power factor on the grid side in relation to the selected target. The reference current for controlling the converter is extracted from the power by inversing the transform in (32). The last stage of the control system is the proportional–integral current controller and the pulsewidth modulation unit.

IV. CASE STUDY AND SIMULATION

In this section, a case study is presented to verify the analysis and the comprehensive design procedure developed in the previous sections. The circuit schematics can be found in Fig. 9. The traction substation uses one single-phase traction transformer. Its primary side is connected to a 110-kV power network, and its secondary side provides a 27.5-kV supply to the traction loads. The traction load is 15 MVA, with a load power factor of 0.85. The system source impedance is calculated as 2 mH according to the short-circuit capacity of the common traction power supply of 750 MVA.

Simulation models are built using PSCAD/EMTDC. Table I shows the practical on-site data for the harmonic distribution in the traction load for the Wuqing substation in China [25]. The load harmonics are designed according to the data in Table I. The grid-side voltages and currents without the HRPC are shown in Fig. 10, which shows that the traction load currents

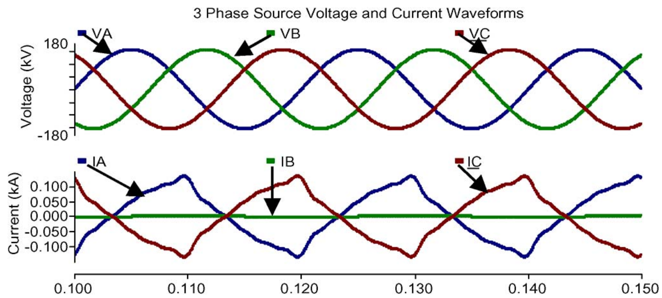

Fig. 10. Grid-side voltage and current waveforms without the HRPC.

TABLE II
PARAMETER DESIGN FOR THE HRPC

No.	Items	Full	Partial
1	Traction transformer	190 kV/27.5 kV	
2	β-phase Coupling Transformer	190 kV/9 kV	
3	k k_α k_β	0.5 0.2887 0.5774	0.2154 0.1640 1.1182
4	α-phase Coupling Inductor L_α	6.6 mH	9.3 mH
5	α-phase Coupling Capacitor C_α	61.00 uF	43.45 uF
6	β-phase Coupling Inductor L_β	8 mH	10 mH
7	V_{dc}	18.7 kV	11 kV
8	Sampling frequency	20 kHz	

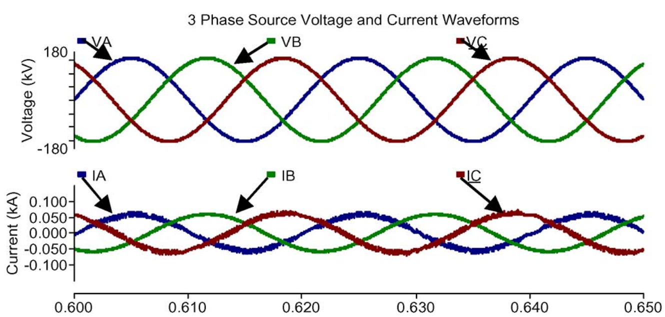

Fig. 11. Grid-side voltage and current waveforms with the HRPC settings for achieving full compensation ($V_{\mathrm{dc}} = 18.7$ kV).

are severely unbalanced with a low power factor and high harmonics contents.

An HRPC is installed to improve the power quality of the Wuqing substation in simulation. The parameters designed for the HRPC with full compensation are listed in Table II. Full compensation is first achieved by the HRPC using a dc-link voltage of 18.7 kV. The grid-side voltages and currents after compensation are shown in Fig. 11. The three-phase currents are balanced with the unity power factor. The harmonics are also eliminated. The system performance is summarized in Table III, in which the HRPC rating is calculated by

$$S_{\mathrm{HRPC}} = S_\alpha + S_\beta = \frac{V_{\mathrm{dc}}}{\sqrt{2}}(I_{c\alpha} + I_{c\beta}). \qquad (34)$$

The target for the partial compensation is set according to the utility tariff plan for the reactive power. For example, the power factor must be at least 0.9 to avoid a penalty [26]. For the traction motor, more reactive power is consumed during the motor starting. It is better to overdesign the reactive power compensation capability. A safety margin is required to take into account possible overloading. In this paper, 0.95 is used as

TABLE III
SYSTEM PERFORMANCE IN THE SIMULATION

Condition	Power Factor	Source Current THD (phase A)	Current Unbalance	Voltage Unbalance	HRPC Rating (MVA)
Before Compensation	0.60	14.7%	100%	2.59%	---
HRPC with full compensation(V_{dc}=18.7 kV)	0.997	2.34%	4.75%	0.40%	15.13
HRPC with full compensation(V_{dc}=11kV)	0.985	37.9%	22.63%	0.84%	10.5
HRPC with partial compensation(V_{dc}=11 kV)	0.954	3.27%	44%	1.03%	6.97

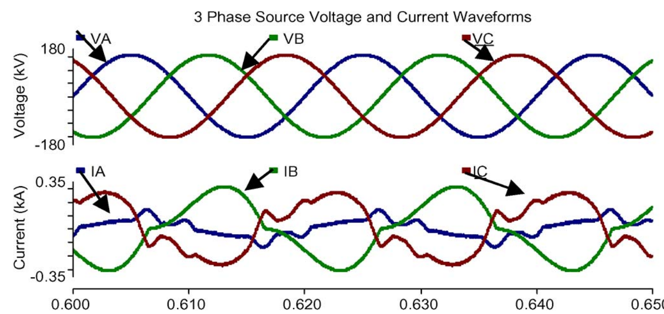

Fig. 12. Unsatisfactory grid-side voltage and current waveforms under a reduced voltage with the HRPC settings to achieve full compensation ($V_{\mathrm{dc}} = 11$ kV).

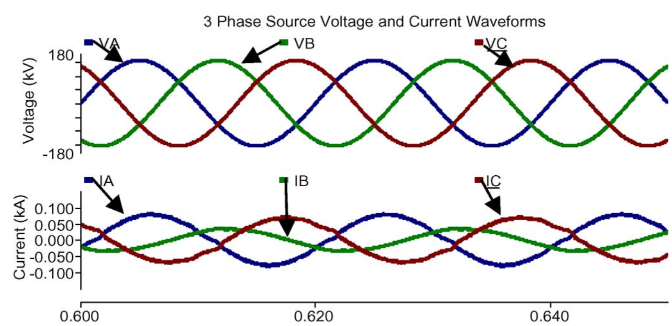

Fig. 13. Grid-side voltage and current waveforms with the HRPC settings to achieve partial compensation (power factor $= 0.95$, $V_{\mathrm{dc}} = 11$ kV).

the power factor to design the HRPC. The system parameters with partial compensation are listed in Table II.

By designing the HRPC with partial compensation, the dc-link voltage is reduced to 11 kV. The HPRC is not able to achieve full compensation under this dc-link voltage. Unsatisfactory grid-side current waveforms are shown in Fig. 12. It is obvious that the HRPC fails to improve the power quality since the reduced dc-link voltage is not high enough for the HRPC to achieve full compensation. The control block diagram shown in Fig. 8 is adopted to modify the reference of the HRPC to achieve partial compensation. The corresponding simulation results are illustrated in Fig. 13 and summarized in Table III. The power factor is improved to around 0.95, and the harmonics are suppressed; the current unbalance is reduced. The voltage unbalance is calculated and given in Table III. The results indicate that the voltage unbalance does not exceed 3% and satisfies the power quality standard [27]. Hence, the current unbalance is compensated for to an acceptable level. The total

TABLE IV
HARMONIC CURRENT CONTENTS IN THE TESTING LOAD

	3rd	5th	7th	9th	11th
Harmonic contents (% of fundamental)	27.9%	5.7%	2.0%	1.5%	1.2%

TABLE V
PARAMETERS DESIGNED FOR THE HRPC IN THE EXPERIMENT

No.	Items	Full	Partial
1	Traction transformer	220 V/50 V	
2	β-phase Coupling Transformer	220 V/25 V	
3	α-phase Coupling Inductor L_α	6.7 mH	6.7 mH
4	α-phase Coupling Capacitor C_α	190 uF	120 uF
5	β-phase Coupling Inductor L_β	10 mH	10 mH
6	V_{dc}	41 V	24 V
7	Sampling frequency	20 kHz	

rating of the HRPC is significantly reduced. It is less than 50% of the rating with full compensation.

V. EXPERIMENTAL RESULTS

A small-capacity HPRC prototype was built with the same system configuration as given in Fig. 9. The peak value of the sinusoidal three-phase supply voltage is 70.7 V. The load comprises a single-phase rectifier, and its harmonic distribution is given in Table IV. The corresponding parameters for the experiment are listed in Table V. The system current and voltage waveforms are monitored using a Yokogawa DL750 16 channel ScopeCorder oscilloscope, and the power quality is recorded using a Fluke 43B Power Quality Analyzer.

The voltage and current waveforms at the grid side are shown in Fig. 14(a) when only a single-phase transform supplies the load. The HRPC is first controlled to do full compensation. The system waveforms with the HRPC under full compensation are presented in Fig. 14(b). It can be concluded in Fig. 14(a) and (b) that the current unbalance, the reactive power, and the harmonics are compensated for simultaneously. The system performance is summarized in Table VI. The dc-link voltage under this case is 41 V, which is lower than the grid-side voltage.

The HRPC is tested by adjusting the compensation target. The power factor is set to 0.95, and the parameters in the control blocks are modified accordingly. The waveforms with the HRPC under partial compensation are presented in Fig. 14(c). The dc-link voltage is reduced to 24 V. The reactive current and the unbalance are partially compensated for. The harmonics are eliminated, as illustrated in Fig. 14 and Table VI. With sufficient short-circuit capacity, the power quality standard is satisfied. A converter rating reduction of more than 50% is achieved with partial compensation. Not only is the initial cost of the system reduced, the operational losses are also reduced as the dc-link operating voltage is lower.

VI. CONCLUSION

An HRPC is applied to a conventional traction power supply system, which uses single-phase traction transformers to supply nonlinear traction loads. The HRPC is applied to reduce reactive power, relieve system unbalance, and suppress harmonics. Partial compensation is implemented to reduce the compensating current and operational voltage of the HRPC. A comprehensive design procedure is proposed for the HRPC to reduce the converter rating with partial compensation. With the proposed design method, the rating of the HRPC is expressed as a function of the power factor at the grid side. For example, the HRPC rating decreases by 50% if the grid-side power factor is set to 0.95 instead of to unity. The initial cost and size of the system are greatly reduced. The control system of the HRPC with partial compensation is implemented. The design and control of the HRPC with partial compensation are verified by simulation. A small-capacity experimental prototype is built in the laboratory, and testing results are also provided to verify the design and control method.

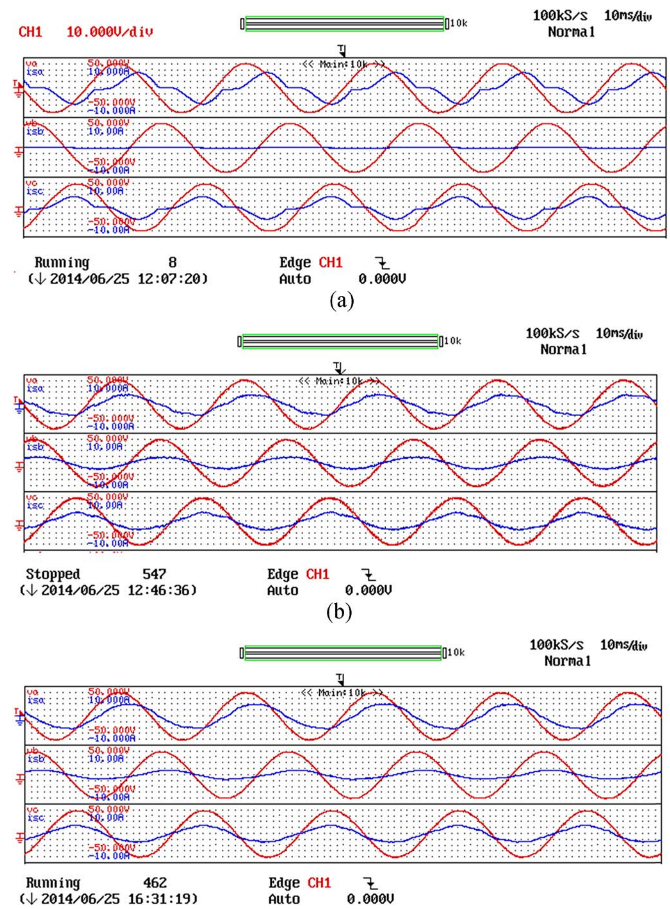

Fig. 14. Experimental results: the three-phase voltage and current at the grid side. (a) Without HRPC. (b) HRPC with full compensation. (c) HRPC with partial compensation.

TABLE VI
SYSTEM PERFORMANCE IN THE EXPERIMENT

Condition	Power Factor	Source Current THD(phase A)	Current Unbalance	HRPC Rating
Before Compensation	0.76	28.6%	92.2%	---
HRPC with full compensation	0.95	9.1%	26%	142.3 VA
HRPC with partial compensation	0.94	6.9%	43.3%	62.97 VA

REFERENCES

[1] Y. Jiang, J. Q. Liu, W. Tian, M. Shahidehpour, and M. Krishanurthy, "Energy harvesting for the electrification of railway stations," *IEEE Electrification Mag.*, vol. 2, no. 3, pp. 39–48, Sep. 2014.

[2] A. Gomez-Exposito, J. M. Mauricio, and J. M. Maza-Ortega, "VSC-based MVDC railway electrification system," *IEEE Trans. Power Del.*, vol. 29, no. 1, pp. 422–431, Feb. 2014.

[3] P.-C. Tan, P. C. Loh, and D. G. Holmes, "Optimal impedance termination of 25-kV electrified railway systems for improved power quality," *IEEE Trans. Power Del.*, vol. 20, no. 2, pp. 1703–1710, Apr. 2005.

[4] S. T. Senini and P. J. Wolfs, "Novel topology for correction of unbalanced load in single phase electric traction systems," in *Proc. IEEE PESC*, Cairns, Australia, Jun. 2002, vol. 3, pp. 1208–1212.

[5] Y. Q. Liu, H. S. Hua, G. P. Wu, and L. Wang, "Research for the effects of high-speed electrified railway traction load on power quality," in *Proc. DRPT*, 2011, pp. 569–573.

[6] H. Wang, Y. Tian, and Q. Gui, "Evaluation of negative sequence current injection into the public grid from different traction substation in electrical railways," in *Proc. Int. CIRED*, 2009, pp. 1–4.

[7] B. Fukala and J. Palecek, "Comparison of schemes of traction transformer stations in terms of their impact on the asymmetry in the power supply system," in *Proc. 15th Int. Conf. EPE*, 2014, pp. 207–210.

[8] G. Lin, X. Yonghai, X. Xiangnin, L. Yingying, and J. Peisi, "Analysis of adverse effects on the public power grid brought by traction power-supply system," in *Proc. IEEE Electr. Power Energy Conf.*, pp. 1–7.

[9] T. Tanaka, K. Ishibashi, N. Ishikura, and E. Hiraki, "A half-bridge inverter based active power quality compensator for electrified railway," in *Proc. Int. Power Electron. Conf.*, 2010, pp. 1590–1595.

[10] Z. Shu, L. Xie, and Q. Li, "Single-phase back-to-back converter for active power balancing, reactive power compensation and harmonic filtering in traction power system," *IEEE Trans. Power Electron.*, vol. 26, no. 2, pp. 334–343, Feb. 2011.

[11] G. Zhu, J. Chen, and X. Liu, "Compensation for the negative-sequence currents of electric railway based on SVC," in *Proc. ICIEA*, 2008, pp. 1958–1963.

[12] J. Ma, M. Wu, and S. Yang, "The application of SVC for the power quality control of electric railways," in *Proc. SUPERGEN*, 2009, pp. 1–4.

[13] Q. Wu, Q. Jiang, and Y. Wei, "Study on railway unified power quality controller based on STATCOM technology," in *Proc. PEOCO*, 2011, pp. 297–300.

[14] Y. Horita *et al.*, "Single-phase STATCOM for feeding system of ToKaido Shinkansen," in *Proc. IPEC*, 2010, pp. 2165–2170.

[15] W. Hosny, H. E. Park, and J. H. Song, "Investigation of shunt active power filters in railway systems, substation installation," in *Proc. EPQU 2011*, 2011, pp. 1–6.

[16] X. Z. Xu, B. C. Chen, and F. C. Gan, "Electrical railway active power filter research based on genetic algorithms," *Proc. ICCA*, 2007, pp. 1465–1468.

[17] T. Uzuka, "Faster than a speeding bullet: An overview of Japanese high-speed rail technology and electrification," *IEEE Electrification Mag.*, vol. 1, no. 1, pp. 11–20, Sep. 2013.

[18] Z. Shu *et al.*, "Digital Detection, control, and distribution system for co-phase traction power supply application," *IEEE Trans. Ind. Electron.*, vol. 60, no. 5, pp. 1831–1839, May 2013.

[19] X. He *et al.*, "Advanced cophase traction power supply system based on three-phase to single-phase converter," *IEEE Trans. Power Electron.*, vol. 29, no. 10, pp. 5323–5333, Oct. 2014.

[20] B. Gholizad and M. Akhbari, "A topology of hybrid active power filter for simultaneously compensating harmonics and load unbalance in single phase traction systems," in *Proc. Conf. Power Eng., Energy Electr. Drives*, 2011, pp. 1–6.

[21] K.-W. Lao, N. Dai, W. G. Liu, and M. C. Wong, "Hybrid power quality compensator with minimum DC operation voltage design for high speed traction power systems," *IEEE Trans. Power Electron.*, vol. 28, no. 4, pp. 2024–2036, Apr. 2013.

[22] N. Y. Dai, K.-W. Lao, M-C. Wong, and C.-K. Wong, "Hybrid power quality conditioner for co-phase power supply system in electrified railway," *IET Power Electron.*, vol. 5, no. 7, pp. 1084–1094, Aug. 2012.

[23] K.-W. Lao, M-C. Wong, N. Y. Dai, C.-K. Wong, and C.-S. Lam, "A systematic approach to hybrid railway power conditioner design with harmonic compensation," *IEEE Trans. Ind. Electron.*, vol. 62, no. 2, pp. 930–942, Feb. 2015.

[24] N. Y. Dai, M-C. Wong, K.-W. Lao, and C.-K. Wong, "Modelling and control of a railway power conditioner in co-phase traction power system under partial compensation," *IET Power Electron.*, vol. 7, no. 5, pp. 1044–1054, May 2014.

[25] K. Yu, *Electric Railway Power Supply and Power Quality*. Beijing, China: China Electr. Power Press, 2010.

[26] *Quality of Electric Energy Supply Admissible Three-Phase Voltage Unbalance Factor*, National Standards of the People's Republic of China, GB/T 15543-1995.

[27] *IEEE Recommended Practice for Monitoring Electric Power Quality*, IEEE Std 1159-2009, Jun. 26, 2009.

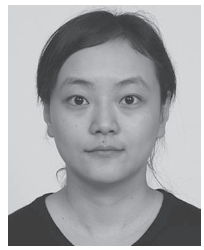

Ning Yi Dai (S'05–M'08) was born in Jiangsu, China. She received the B.Sc. degree in electrical engineering from Southeast University, Nanjing, China, in 2001 and the M.Sc. and Ph.D. degrees in electrical and electronics engineering from the University of Macau, Macau, China, in 2004 and 2007, respectively.

She is currently an Assistant Professor with the Department of Electrical and Computer Engineering, Faculty of Science and Technology, University of Macau. She is the author or coauthor of more than 40 technical journal and conference papers in the field of power systems and power electronics. Her research interests include the application of power electronics in power systems, renewable energy integration, and pulsewidth modulation.

Dr. Dai was the corecipient of the Macao Science and Technology Invention Award (Third Class) in 2012.

Keng-Weng Lao (S'09) was born in Macau, China, in 1987. He received the B.Sc. and Master's degrees in electrical and electronics engineering from the University of Macau, Macau, China, in 2009 and 2011, respectively. He is currently working toward the Ph.D. degree in the Department of Electrical and Computer Engineering, Faculty of Science and Technology, University of Macau.

His research interests include flexible alternating-current transmission system compensation devices, energy saving, and renewable energy.

Mr. Lao was the recipient of the Challenge Cup National Inter-Varsity Science and Technology Competition (first runner-up) in China and the Championship of the Postgraduate Section in The Institution of Engineering and Technology Young Professionals Exhibition and Competition in Hong Kong in 2013. He was also the recipient of the Champion Award of the Schneider Electric Energy Efficiency Cup in Hong Kong in 2010.

Chi-Seng Lam (S'04–M'12) received the B.Sc., M.Sc., and Ph.D. degrees in electrical and electronics engineering from the University of Macau (UM), Macau, China, in 2003, 2006, and 2012, respectively.

From 2006 to 2009, he was an Electrical and Mechanical Engineer with the Campus Development and Engineering Section, UM. In 2009, he returned to the Power Electronics Laboratory, Faculty of Science and Technology, UM, to work as a Technician, and at the same time, he started to pursue his Ph.D. studies. In 2013, he was a Postdoctoral Fellow with The Hong Kong Polytechnic University, Hung Hom, Hong Kong. He is currently an Assistant Professor with the State Key Laboratory of Analog and Mixed-Signal VLSI, Faculty of Science and Technology, UM. He is the coauthor of the book *Design and Control of Hybrid Active Power Filters* (Springer, 2014) and of more than 40 technical journal and conference papers. He is the holder of two Chinese patents. His research interests include integrated power electronics controllers, power management integrated-circuit design, power quality compensators, electric vehicle chargers, and renewable energy.

Dr. Lam was the GOLD Officer and Student Branch Officer of the IEEE Macau Section in 2007 and 2008, respectively. He is currently the Secretary of the IEEE Macau Section and the IEEE Macau Power and Energy Society/IEEE Power Electronics Society Joint Chapter. He was the corecipient of the Macao Science and Technology Invention Award (third class) in 2014. He was also the recipient of the Macao Science and Technology Research and Development Award for Postgraduates (Ph.D. level) in 2012 and the Third Regional Inter-University Postgraduate Electrical and Electronic Engineering Conference Merit Paper Award in 2005.